

Supporting information

Polymorphs and Isostructural Cocrystals of Dexamethasone: Towards the improvement of aqueous solubility

Richu Bagya Varsa S^a, Palash Sanphui,^{*a} Vladimir Chernyshev^{*b,c}

^aDepartment of Chemistry, Faculty of Engineering and Technology, SRM Institute of Science and Technology, Chennai, Tamil Nadu 603203, India. E-mail: palashi@srmist.edu.in

^bDepartment of Chemistry, M. V. Lomonosov Moscow State University, 1-3 Leninskie Gory, Moscow 119991, Russian Federation. E-mail: vladimir@struct.chem.msu.ru

^cA. N. Frumkin Institute of Physical Chemistry and Electrochemistry RAS, 31 Leninsky Prospect, Moscow 119071, Russian Federation

Table of contents

1. Table S1. Hydrogen bond geometry.....	
2. Table S2. Summary of the reported steroid cocrystals/salts structure.....	
3. Fig. S1. Polarized microscope images of DEX concomitant polymorphs.....	
4. Fig. S2. TGA endotherms of DEX–CAT and DEX–RES cocrystals.....	
4. Fig. S3. Packing differences between Forms A and B.....	
5. Fig. S4. Overlay of molecular conformations of DEX polymorphs.....	
6. Fig. S5. The Rietveld plots of (a) DEX–CAT and (b) DEX–RES cocrystals.....	
7. Fig. S6. 3D packing view of (a) DEX–CAT and (b) DEX–RES cocrystals.....	
8. Fig. S7. X-ray powder pattern of (a) DEX+ORC, (b) DEX+PYR, (c) DEX+PGL ground mixture.	
9. Fig. S8. H-bonding aspects of (a) progesterone-resorcinol (refcode-PRORES), (b) DEX-RES...	
10. Fig. S9. UV absorbance spectra of the DEX Forms A/B and DEX-CAT/RES cocrystals..	
11. Fig. S10. XRD comparison of DEX–CAT/RES cocrystals following 2h dissolution.....	
12. Fig. S11. XRD comparison of DEX–CAT/RES cocrystals under humidity conditions.....	

Table S1. Hydrogen bond geometry (Å, °)

DEX (Form A)	D-H...A	D-H/ Å	H...A/Å	D...A/Å	D-H...A/°	Symmetry code
	O2-H2...O1	0.82	2.17	2.6395(2)	116	Intramolecular
	O3-H3...O5	0.82	2.17	2.9383(2)	155	x,1+y,z
	O4-H4...O2	0.82	2.19	3.0076(2)	146	-x,-1/2+y,1/2-z
	C18-H18B...O4	0.96	2.24	2.8762(2)	123	Intramolecular
DEX (Form B)	O1-H1...O10	0.82	2.15	2.9366(3)	160	3/2-x,1-y,-1/2+z
	O4-H13...O9	0.82	2.07	2.8230(3)	153	1/2+x,1/2-y,-z
	O6-H30...O3	0.82	1.99	2.7821(3)	163	3/2-x,1-y,-1/2+z
	O8-H36...O2	0.82	2.02	2.8138(3)	163	-1/2+x,1/2-y,-z
	C17-H17...O10	0.97	2.49	3.2999(3)	141	3/2-x,1-y,-1/2+z
	C21-H26...O7	0.96	2.54	3.4414(3)	156	1+x,y,z
	C39-H48...O3	0.97	2.52	3.3143(3)	139	3/2-x,1-y,-1/2+z
DEX-CAT	O3-H3...O5	0.82	2.07	2.8475(4)	158	x,y,-1+z
	O6-H6...O7	0.82	2.21	2.9416(4)	149	1-x,1/2+y,1-z
	O7-H7...O2	0.82	1.81	2.5987(3)	162	1-x,-1/2+y,-z
	O2-H2...O1	0.82	2.14	2.6277(3)	118	Intramolecular
DEX-RES	O3-H3...O5	0.82	2.26	3.0598(4)	164	x,y,1+z
	O6-H6...O6	0.82	2.58	3.2285(4)	137	-x,1/2+y,1-z
	O7-H7...O2	0.82	2.20	3.0111(4)	168	x,-1+y,z
	C5-H5A...O5	0.96	2.46	2.8623(4)	105	x,y,1+z
	C5-H15A...O5	0.97	2.60	3.5411(5)	163	1-x,-1/2+y,-z
	C24-H24...O2	0.93	2.47	3.2569(4)	142	x,-1+y,z

	C26-H26...O7	0.93	2.34	3.1443(4)	144	-x,1/2+y,2-z
--	--------------	------	------	-----------	-----	--------------

Table S2. Steroid cocrystals/salts structure (reported)

Sl. No	Steroid	Coformer used with CCDC refcodes/nos	References
1.	Nandrolone	Salicylic acid (LUYHAR), 3-Amino-1,2,4-Triazole (LUYHEV)	Iqbal et al., J. Mol. Struct. 2021, 1224, 128981. DOI: 10.1016/j.molstruc.2020.128981
2.	Diosgenin	Piperazine (PACVEY)	Gong et al., Natural Products and Bioprospecting 2020, 10, 261–267. DOI: 10.1007/s13659-020-00256-y
3.	Cholic acid	Melamine (TALDIV)	Ikonen et al., CrystEngComm 2010, 12, 4304. DOI: 10.1039/c0ce00108b
4.	Stanozolol	Malonic acid (VOPCOU), Phenylacetic Acid (VOPFAJ), 6-Hydroxy-2-Naphthoic Acid (VOPCUA).	Norberg et al., Cryst. Growth Des. 2014, 14, 7, 3408–3422 DOI: 10.1021/cg500358h
		Saccharin (salt/EYAYOU), Acesulfame (salt/EYAYUA)	Kong et al., CrystEngComm, 2016,18, 8739-8746 DOI: 10.1039/C6CE01876A
		2,5-dihydroxybenzoic acid (JIWJEH), 2,6- dihydroxybenzoic acid (salt/JIWJAD), Phthalic Acid (JIWJIL), Gallic acid (salt/JIWJAD).	Wang et al., CrystEngComm, 2019, 21, 2144 DOI: 10.1039/c8ce01439f
5.	Estradiol	Benzoquinoline (RUFYIC), 1,2-Dimethylnaphthalene (RUFYOI), Phenanthrene (RUGYID) Pyrene (CUTBEZ) Urea (ESOURE10) Isonicotinamide (ULUFIS) Piperazine (ULUFOY) Perfluoronaphthalene (RUGYEZ)	Ardila-Fierro et al. Cryst. Growth & Des. 2015, 15, 1492-1501. DOI: 10.1021/cg501865h
6	Ethinyl estradiol	Nicotinamide, Piperazine, Tetramethylpyrazine, 4,4'-bipyridine Imidazole (CCDC nos 1938507-11)	Du et al., New J. Chem., 2019, 43, 16889-16897 DOI: 10.1039/C9NJ04147H
7	Estradiol	Urea (ESOURE10)	Duax et al. Acta Cryst. B, 1972, 28, 1864-1871, DOI: 10.1107/S0567740872005151

		Acetamide (CCDC no.: 1910680)	Gong e al., Zeitschrift für Kristallographie- New Crystal Structures, 2020, 235, 31-34. DOI: 10.1515/ncrs-2019-0451
		Isonicotinamide (ULUFIS) Piperazine (ULUFOY)	Wang et al., CrystEngComm, 2016,18, 3498-3505 DOI: 10.1039/C6CE00433D
8	Progesterone	9-phenanthrol (CUSZAS), Gentisic acid (CUSZIA), 2,7-dihydroxynaphthalene (CUSZEW), 4-bromophenol (CUSYOF)	Friscic et al., Proc. Nat. Acad. Sci. USA 2010, 107, 13216, DOI: 10.1073/pnas.0915142107
		4-hydroxybenzoic acid (CCDC nos 1571644-5)	Samipillai et al., J. Crystal Growth 2019, 507, 270-282. DOI: 10.1016/j.jcrysgro.2018.10.050
		Phloroglucinol (YUKQAZ/YUKVAZ), Resveratrol (YUKQED)	Guo et al., Cryst. Growth Des. 2020, 20, 3053–3063 DOI: 10.1021/acs.cgd.9b01688
		Hydroquinone (KEFBEC)	Galdecki et al., J. Crystallogr. Spectrosc. Res., 1989, 19, 983-991. DOI: 10.1007/BF01160880
		Resorcinol (PRORES)	Dideberg et al., Acta Crystallogr., 1975, B31, 637-640, DOI: 10.1107/S0567740875003524
		Pregnenolone (TIPMAH)	Lancaster et al., J. Pharm. Sci., 2007, 96, 3419-3431. DOI: 10.1002/jps.20983
9	Pregnenolone	4-iodophenol (WOMGOV) 2,4,6-trichlorophenol (CCDC 687158)	Bhatt et al., CrystEngComm 2008, 10, 1747-1749. DOI: 10.1039/B810643F
		2-Naphthol (CUTBAV) 4-bromophenol (CUTBOJ)	Friscic et al., Proc. Nat. Acad. Sci. USA 2010, 107, 13216, DOI: 10.1073/pnas.0915142107
10	Cholesterol	4-iodophenol (WOMHAI)	Bhatt et al., CrystEngComm 2008, 10, 1747-1749. DOI: 10.1039/B810643F
11	β -sitosterol	Propionic acid, Zymonic acid, Gallic acid (ZUQJON), 4-hydroxybenzoic acid, 3,4-dihydroxybenzoic acid.	Barbas et al., CrystEngComm, 2020, 22, 4210-4214 DOI: 10.1039/D0CE00704H
12	Exemestane	1-hydroxypyrene (KURBUX/KURCAE) 9-hydroxyphenanthrene (KURBOR)	Topić et al., Canadian J. Chem. 2020, 98, 386-393. DOI: 10.1139/cjc-2020-0073
		Thiourea (CCDC nos 1970916-7)	Fatima et al., IUCrJ 2020, 7, 105-112 DOI: 10.1107/S2052252519016142

		Maleic acid (HORNAE),	Shiraki et al., Pharm. Res. 2008, 25, 2581–2592. DOI: 10.1007/s11095-008-9676-2
13	Megestrol acetate	Saccharin (HORNEI)	

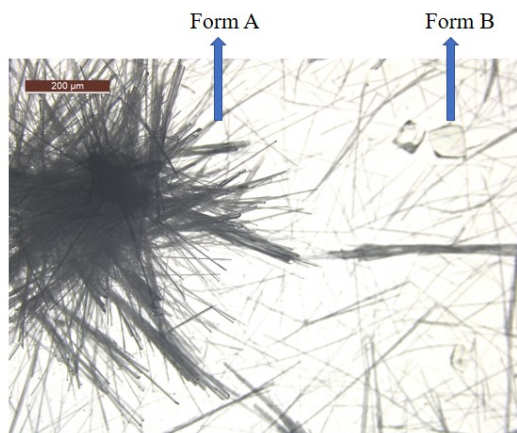
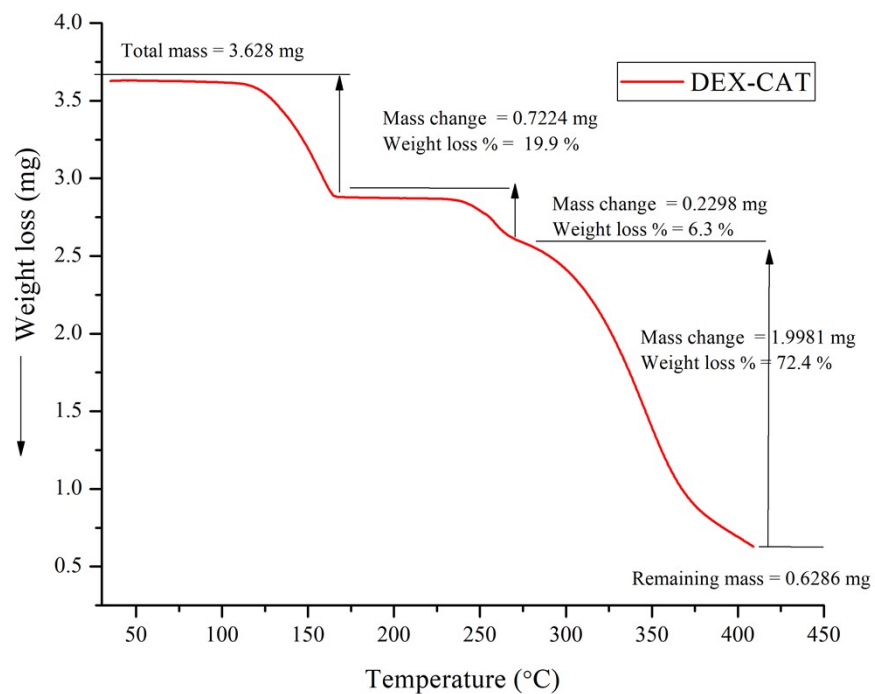
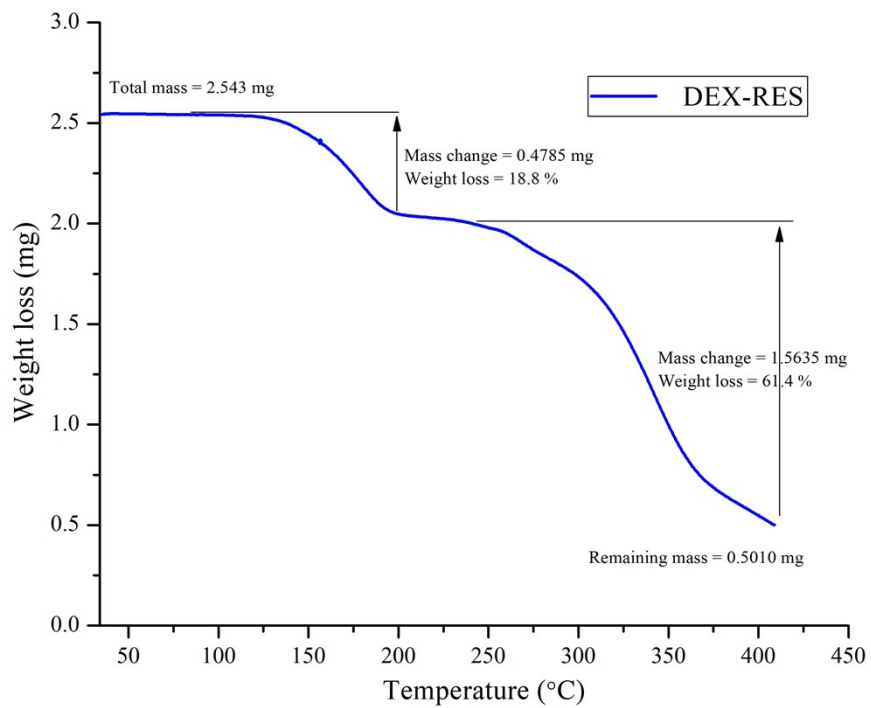


Fig. S1. DEX polymorphs (needle-Form A, square plate-Form B) crystallized concomitantly from acetonitrile.

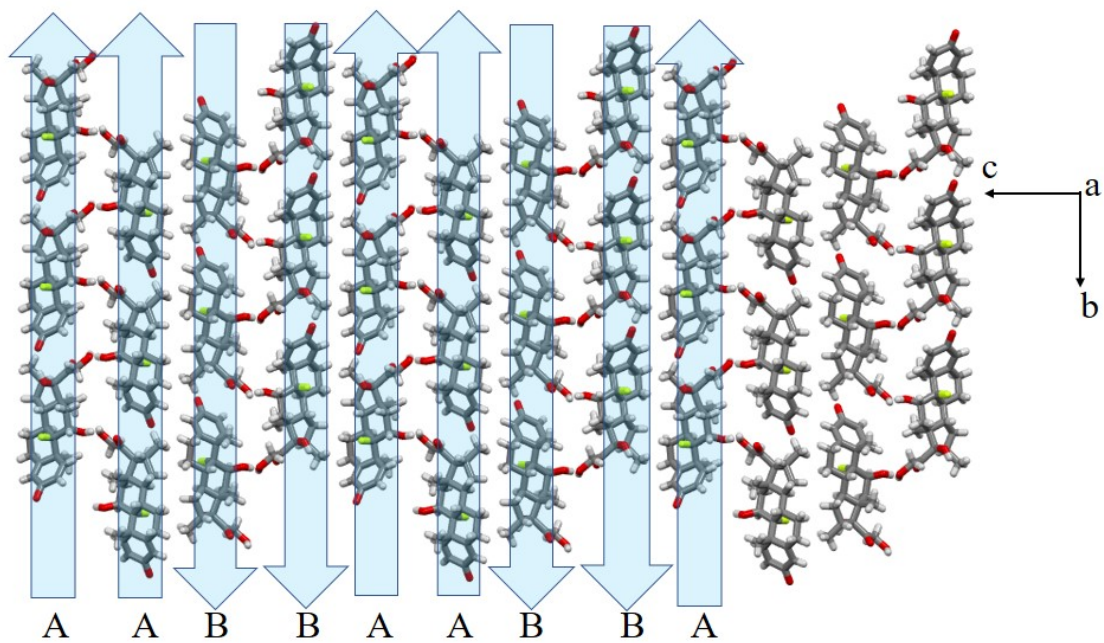


(a)

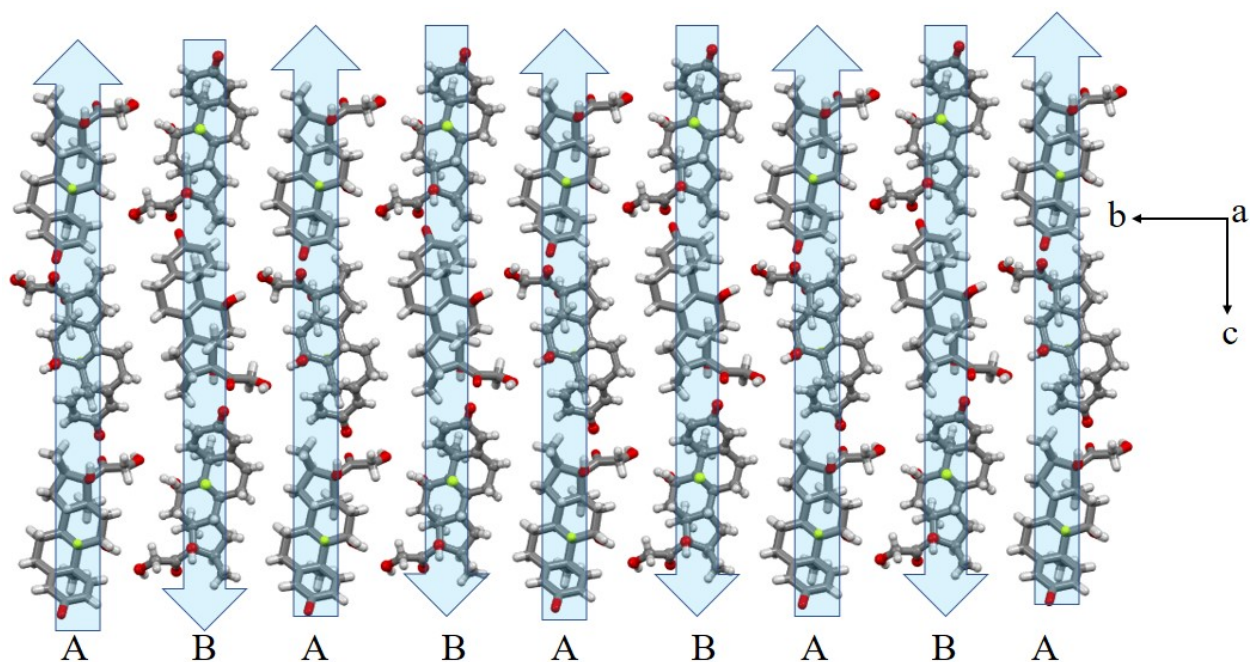


(b)

Fig. S2. TGA data of (a) DEX-CAT and (b) DEX-RES cocrystals confirmed the possible thermal degradation.



(a)



(b)

Fig. S3. Packing differences between Form A and B. Form A maintains AABB patterns, whereas Form B maintains ABAB patterns of DEX chains viewed down the a axis. The direction of arrow is assumed starting from carbonyl towards terminal OH groups as **A**, wherein opposite arrow is assumed as **B**.

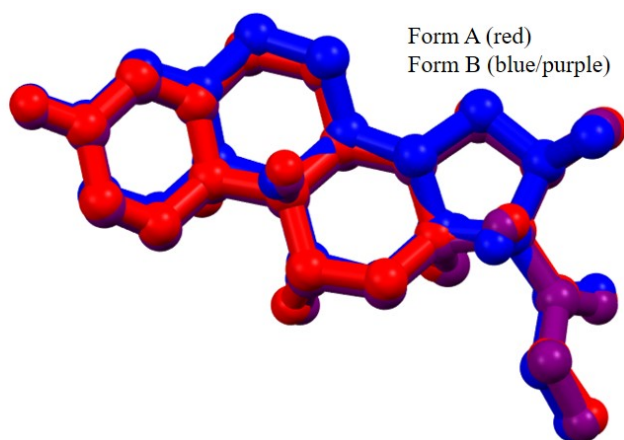
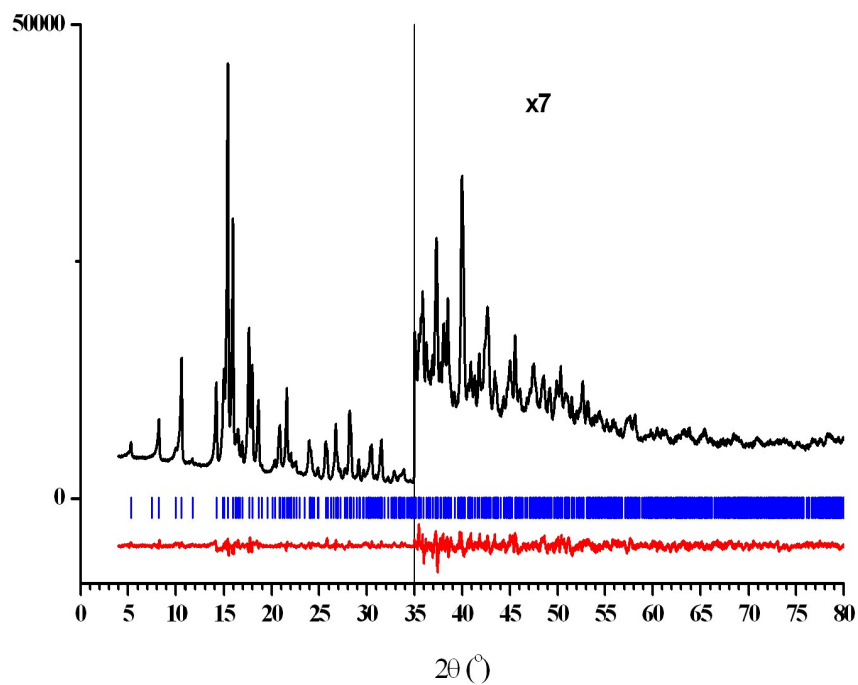
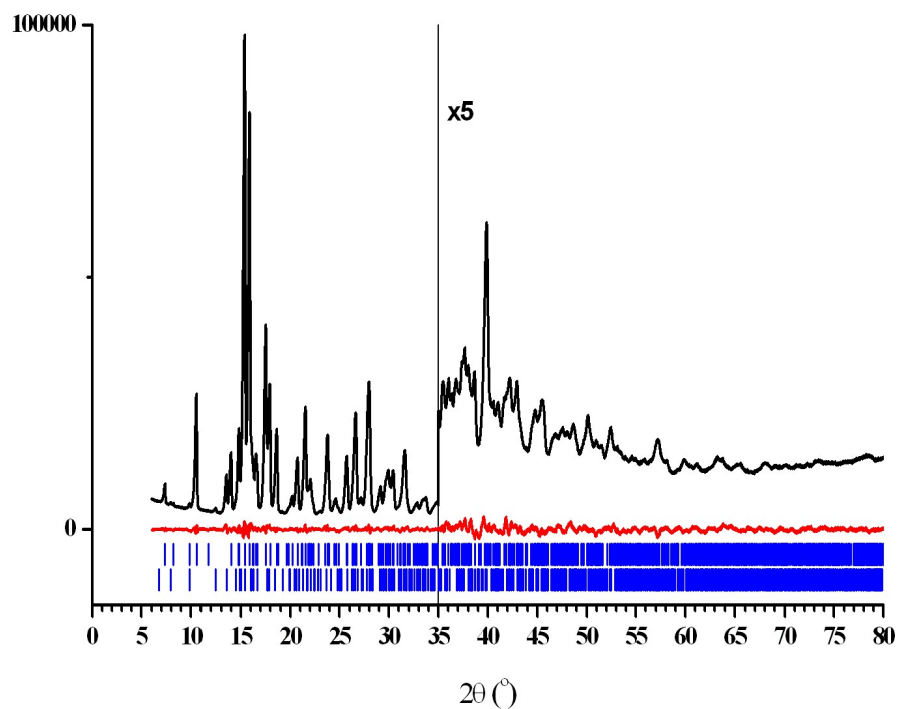


Fig. S4. Overlay of molecular conformations of DEX (three) symmetry independent molecules in two forms A/B that indicates no conformational flexibility even in the presence of eight chiral centers and four aliphatic cyclic rings.



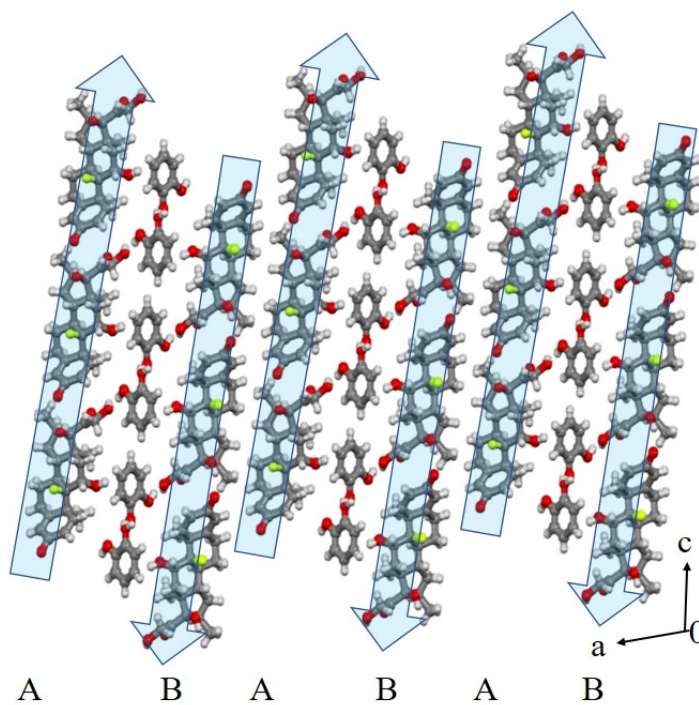
(a)



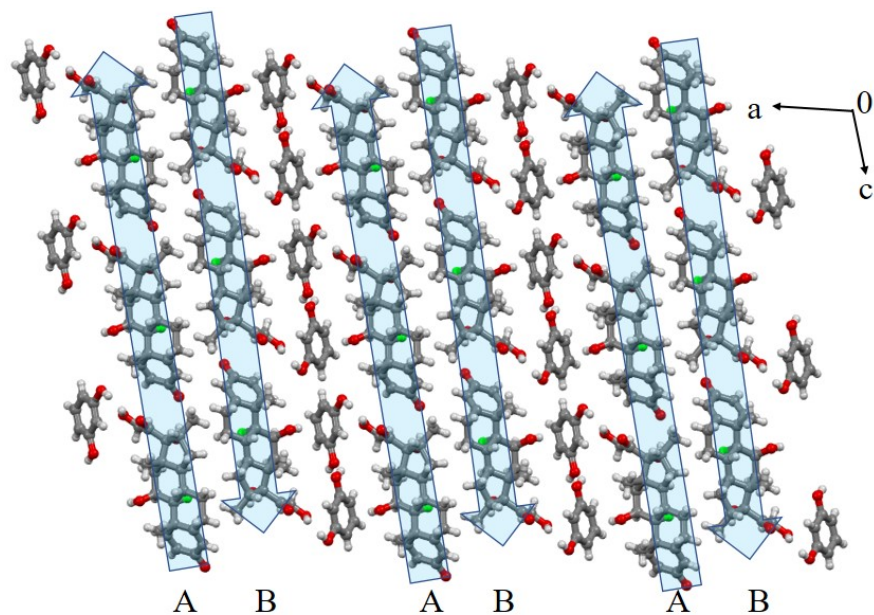
(b)

Fig. S5. The Rietveld plot after the final bond-restrained refinement for (a) DEX-CAT and (b) DEX-RES cocrystals showing the experimental and difference diffraction profiles as black (top) and red (bottom) curves, respectively. The vertical blue bars correspond to the calculated positions of the Bragg peaks.

Note: In the final bond-restrained Rietveld refinement of DEX-RES, two crystalline phases were taken into account, namely, DEX-RES and DEX (Form A). For DEX Form A, the atomic coordinates were fixed to the known values (CCDC deposition 2118348). For DEX-RES, except for the atomic coordinates only two independent *U*_{iso} values for non-H atoms were refined – one common *U*_{iso} for DEX molecule, another one for RES molecule. H atoms were placed in calculated positions and not refined. The experimental and calculated diffraction profiles after the final two-phase bond-restrained Rietveld refinement are shown in Fig. S5b [in the Legend - The vertical blue bars correspond to the calculated positions of the Bragg peaks for two crystalline phases - DEX-RES (1st row) and DEX-Form A (2nd row)]. The content of DEX (Form A) in the DEX-RES sample was estimated as approx. 7%.

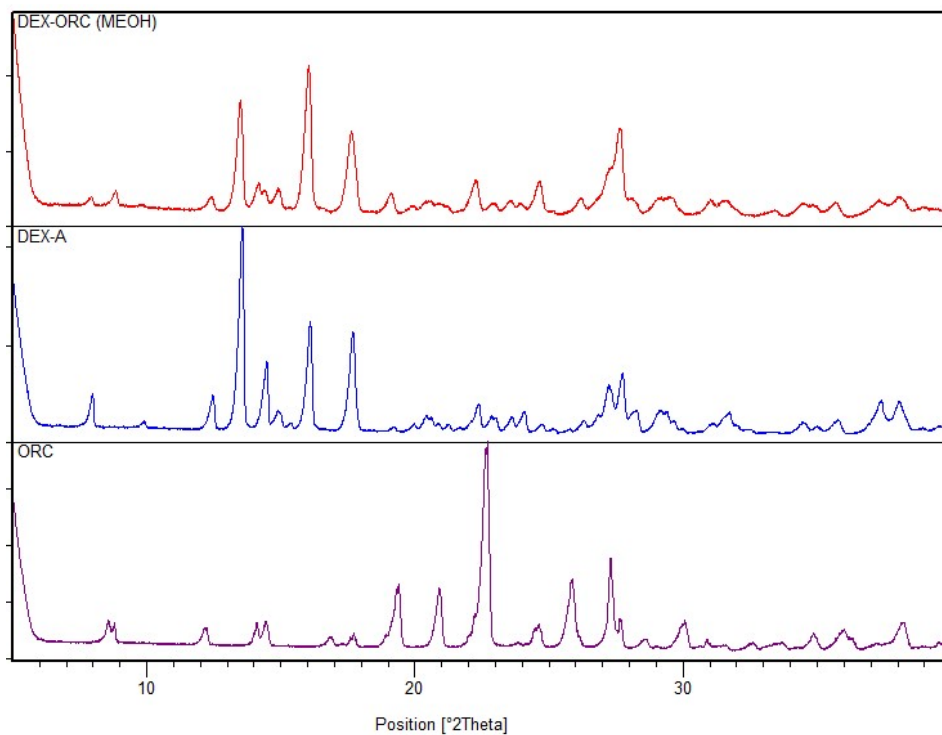


(a)

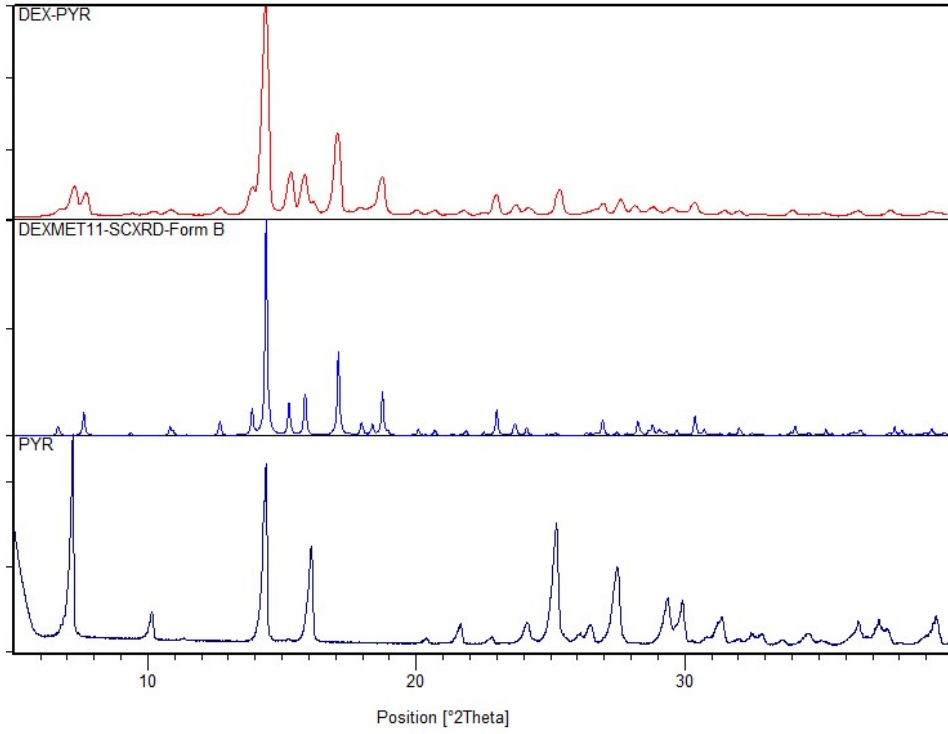


(b)

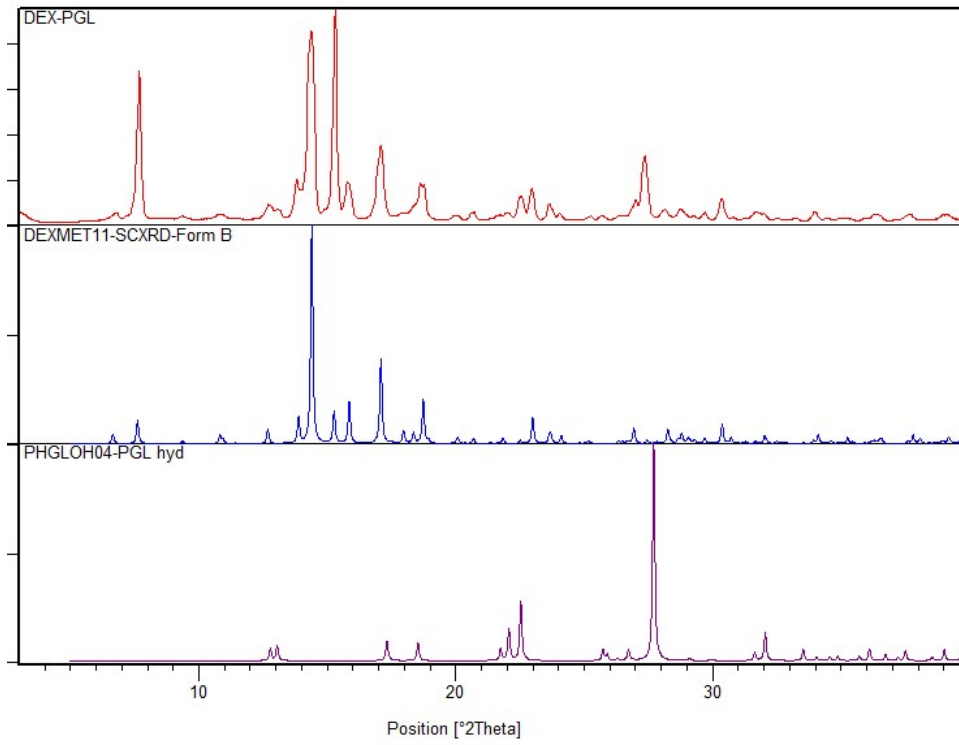
Fig. S6. 3D packing view of (a) DEX–CAT and (b) DEX–RES cocrystals down the *b* axis indicate DEX molecule arranged in an alternate fashion (ABAB), which is similar to DEX Form B.



(a)

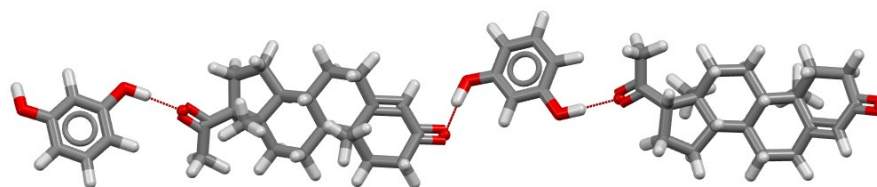


(a)

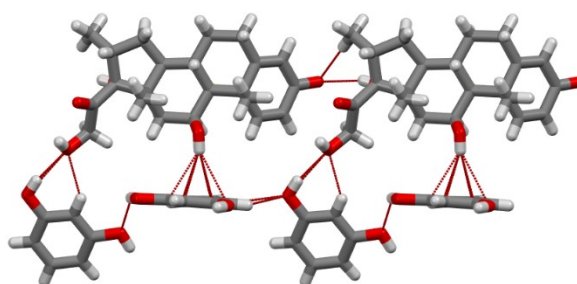


(b)

Fig. S7. X-ray powder pattern of (a) DEX-ORC, (b) DEX-PYR, (c) DEX-PGL suggest that there are two-phase sample of either DEX Form A or Form B (DEXMET11) and PYR/PGL hydrate (PHGLOH04).



(a)



(b)

Fig. S8. Hydrogen bonding aspects of (a) progesterone–resorcinol (refcode-PRORES), (b) DEX–RES cocrystals.

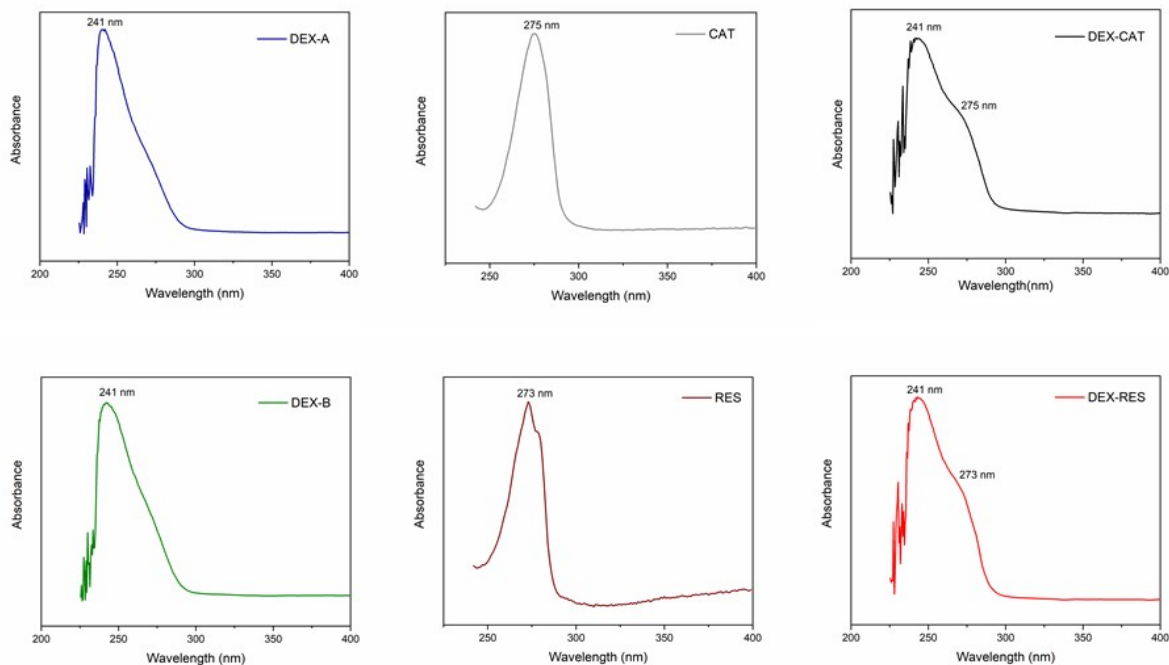
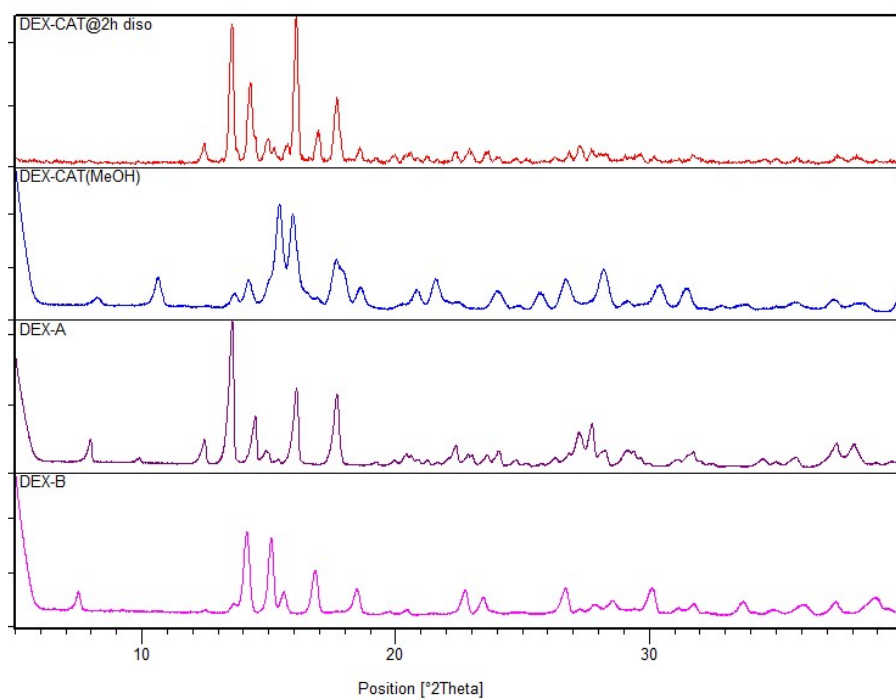
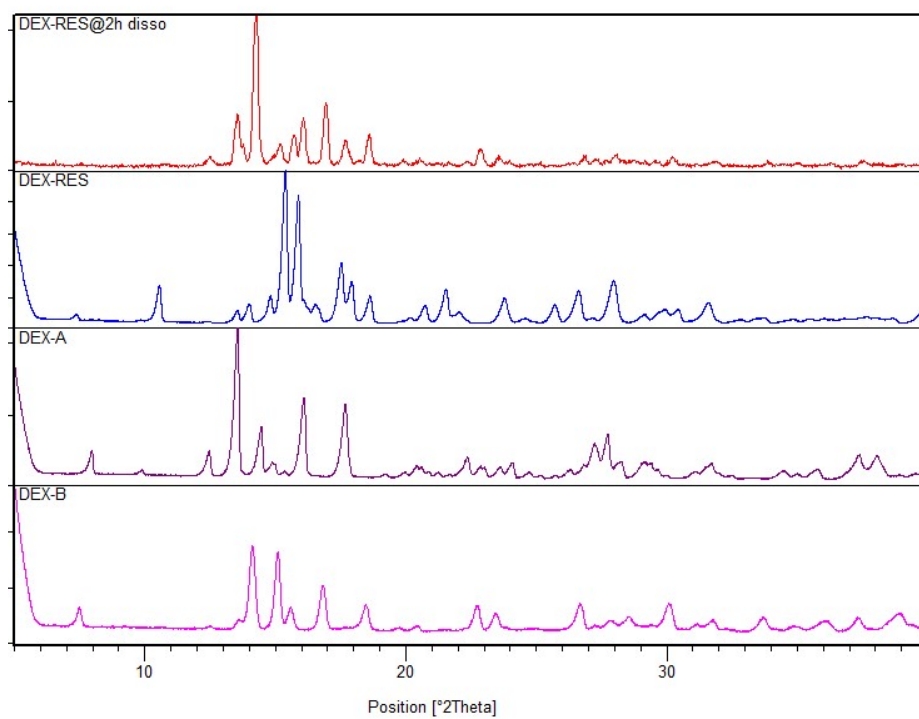


Fig. S9. UV absorbance spectra of the DEX Forms A/B and DEX-CAT/RES cocrystals that showed the negligible interference in the UV region of 241 nm, where the drug is absorbed.

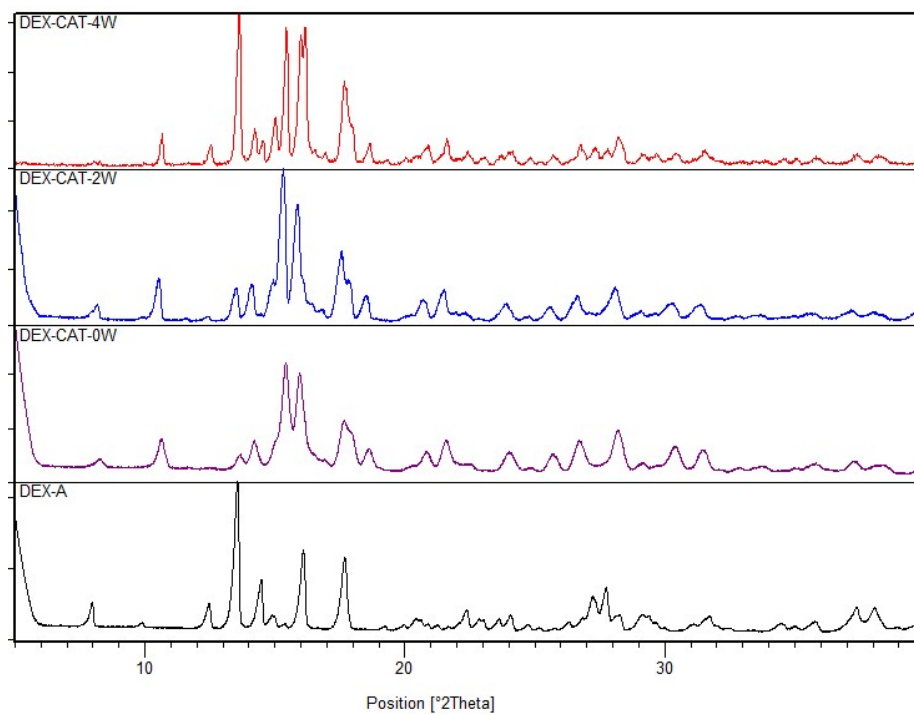


(a)

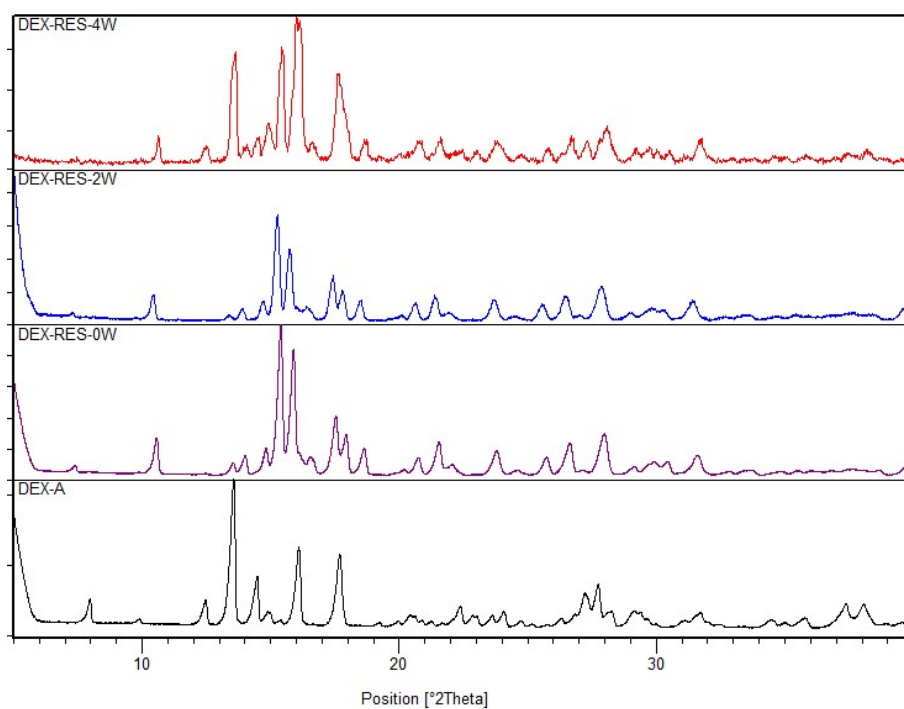


(b)

Fig. S10. XRD comparison of (a) DEX–CAT and (b) DEX–RES cocrystals (following 2h dissolution studies) that indicated the possible transformation to the mixture of polymorphs



(a)



(b)

Fig. S11. XRD comparison of (a) DEX-CAT and (b) DEX-RES cocrystals stored at 35 ± 5 °C and 75% relative humidity that showed partial transformation to DEX Form after 2-4 weeks.